PHILOSOPHICAL MAGAZINE A, 1998, VOL. 78, NO. 5, 1111–1124

Icosahedral quasicrystal formation in Ti–Zr-based alloys and a new classification technique

By W. J. KIM, P. C. GIBBONS and K. F. KELTON

Department of Physics, Washington University, St Louis, Missouri 63130, USA

[*Received 24 July 1997 and accepted in revised form 9 February 1998*]

ABSTRACT

Until recently, icosahedral phase (i-phase) formation was studied primarily in Al–transition metal alloys. The Al-based i-phases generally fall into one of two classes; those believed to be based on the Pauling triacontahedron, fundamental to the Bergman 1/1 phase, and those based on the double-shell Mackay icosahedra found in the 1/1 α-(Al–Mn–Si) phase. Notable Bergman-type quasicrystals include i-(Al–Li–Cu) and i-(Al–Mg–Zn); i-(Al–Mn–Si) forms the best known Mackay-type i-phase. The large number of Ti-based i-phases now known, and the differences in their diffraction features raise the question of their fundamental structural units. To address this partially, results of X-ray and electron microscopy studies of Ti–Zr–Ni alloys, where Ni is replaced by Fe and Co, are reported. The character of the i-phases varies smoothly from the Ti–Zr–Ni quasicrystals, which probably are Bergman-type i-phases, to the Ti–Zr–Fe quasicrystals, which probably are Mackay types. A new classification method for icosahedral quasicrystals based on the ratio of the quasilattice constant a_q to the average atomic separation $\langle a_s \rangle$, computed from the measured density, is introduced and applied to both Al- and Ti-based quasicrystals. On the basis of this scheme, most Ti-based i-phases, including the Ti–3d transition metal–Si–O phases and Ti–Zr–Fe, form a third group, different from the Al-based Mackay and Bergman groups. Ti–Zr–Ni and Ti–Zr–Co quasicrystals fall into the same class as the Bergman-type Al-based i-phases.

§1. INTRODUCTION

Although icosahedral quasicrystal phase (i-phase) formation has been investigated primarily in Al-based alloys (Shechtman *et al.*1984, Sainfort *et al.* 1985, Tsai *et al.* 1989), the Ti and Ti–Zr-based i-phases, which form the second-largest class, are becoming increasingly more interesting. The i-phase has now been reported in Ti–TM–Si–O (Kelton *et al.* 1988, Zhang and Kelton 1990, 1991), Ti–Zr–Ni (Molokanov and Chebotnikov 1990), Ti–Zr–Fe (Kim and Kelton 1995) and Ti–Zr–Co (Kim and Kelton 1996) alloys, where TM indicates one of the 3d transition metals V, Cr, Mn, Fe, Co or Ni. Recently, the first stable non-Al-based quasicrystal, i-(Ti–Zr–Ni) was confirmed in annealed as-cast alloys that initially contained only the C14 hexagonal Laves and Ti–Zr solid-solution phases (Kelton *et al.* 1997).

Selected-area electron diffraction (SAD) patterns taken from the rapidly quenched Ti–TM–Si–O and Ti–Zr–Fe i-phases contain strong disorder-related artefacts, including localized arcs of diffuse scattering and spot shape anisotropy. By contrast, the diffraction patterns taken from rapidly quenched or annealed samples of i-(Ti–Zr–Ni) show none of these artefacts. Interestingly, SAD patterns taken from rapidly quenched samples of i-(Ti–Zr–Co) are intermediate between these two extremes, showing small spot anisotropy and very weak diffuse scattering (Kim

0141-8610/98 $12.00

and Kelton 1996). Such differences in the diffraction patterns among the Ti-based i-phases probably reflect differences in their local-atomic structures.

Owing to the complexity of the quasicrystal structure, the atomic decorations of crystal approximant phases, believed to have similar local atomic configurations as in the quasicrystals, have been studied extensively (Elser and Henley 1985, Audier and Guyot 1986, Libbert *et al.* 1994). Generally, i-phases are classified on the basis of the atomic clusters found in these closely related approximant phases. The bcc 1/1 rational approximants have been particularly well studied. Quasicrystals have been classified by their similarity to either Bergman 1/1 phases, found in Al–Mg–Zn and Al–Li–Cu alloys where the Pauling triacontahedron forms the basic building block, or the Mackay 1/1 phases, found in Al–Mn–Si alloys, which are based on packings of Mackay double-shell icosahedra. Only recently have the appropriate approximants for the Ti-based quasicrystals been identified and refined. The structure of the 1/1 bcc approximant found in Ti–Cr–Si–O alloys (α-(Ti–Cr–Si–O)) was determined by Libbert *et al.* (1994) by X-ray diffraction (XRD) and neutron diffraction. The Ti–Cr–Si–O quasicrystals are related to a Mackay-type 1/1 phase. The structural refinement of the 1/1 bcc approximants of Ti–Zr–Fe (M phase) and Ti–Zr–Ni (W phase) reveals that the M-(Ti–Zr–Fe) is Mackay-type like α-(Ti–Cr–Si–O), while the W-(Ti–Zr–Ni) is Bergman type (Kim *et al.* 1997, 1998b,c). The manner in which the local i-phase structure changes as the alloy composition is varied between two quasicrystal compositions (Ti–Zr–(Ni_xFe_{1-x})) related to two different crystal approximants has not been investigated yet.

There are other clusters found in i-phases and their approximants, for example the pseudo-Mackay cluster of i-(Al–Pd–Mn) (Boudard *et al.* 1992) and the distorted icosahedral clusters in Ti_2Ni or the C14 Laves phase (Stroud 1996). In this work, however, we know from the structures of the 1/1 crystals that the Mackay and the Bergman clusters are the relevant ones. There have been reports recently of other systems in which changes in composition change the clusters found from Bergman to Mackay types (Bresson *et al.* 1998), and of a system in which Bergman and pseudo-Mackay clusters coexist (Beraha *et al.* 1998).

To probe the changes in cluster types with composition further, a series of rapidly cooled alloys was prepared that spanned compositions between the most ordered and the most disordered i-phases: $Ti_{60}Zr_{15}(Fe_{25-x}Ni_x)$, $Ti_{65}Zr_{10}Zr_{10}(Fe_{25-x}Ni_x)$ and $Ti_{53}Zr_{27}(Co_{20-x}Ni_x)$. Results of XRD and electron diffraction studies are reported here. We also report results from a study of the role of atomic size in quasicrystal structures.

Chen *et al.* (1987) suggested that the ratio of the quasilattice constant, a_q (Elser 1985) to the average Goldschmidt diameter $\langle a \rangle$ is approximately 1.65 for Mackay-type quasicrystals. For Bergman-type quasicrystals, $a_q/\langle a \rangle \approx 1.75$. To evaluate the role of atomic size in quasicrystal structure better, we propose a new classification method based on the average atomic separation, which is calculated from the measured i-phase density. This is used to classify the known Ti-based quasicrystals and the series of alloys studied here.

§2. Experimental procedure

Ingots of the desired composition were prepared by arc-melting mixtures of the pure elements in a high-purity Ar gas atmosphere on a water-cooled Cu hearth. These ingots were broken and portions were melt spun in an Ar atmosphere from a zirconia-coated fused silica tube onto a Cu wheel that was rotating with a surface

velocity of 30–70 m s^{-1}. The resulting alloy ribbons were approximately 2 mm wide, 20–45 μm thick and 3–15 cm long. Transmission electron microscopy (TEM) samples were prepared by ion milling in a liquid-N_2-cooled sample stage. A JEOL 2000FX transmission electron microscope equipped with a Noran energy-dispersive X-ray spectrometer was used for microstructural studies, to carry out convergent-beam electron diffraction and SAD studies, and to obtain compositional information. XRD patterns were obtained with a Siemens X-ray diffractometer, using Cu Kα radiation. A computer-controlled Cahn 2000 electronic balance was used to obtain sample densities by the Archimedes weighing technique in toluene.

§3. Results and discussion

In this section, phase formation and changes in quasilattice constant as a function of alloy composition are reported. With measured changes in density and refined structures of 1/1 approximants, these data are used to construct the first classification scheme for Ti-based quasicrystals.

3.1. *Ti–Zr–(Fe–Ni) and Ti–Zr–(Co–Ni) phase formation*

As discussed earlier, two series of alloys were prepared, one varying the Fe-to-Ni ratio while keeping the Ti and Zr concentrations set at two of the best i-phase compositions for Ti–Zr–Fe quasicrystals, namely $Ti_{60}Zr_{15}(Fe_{25-x}Ni_x)$ and $Ti_{65}Zr_{10}(Fe_{25-x}Ni_x)$ (the composition of the stable i-phase is $Ti_{41.5}Zr_{41.5}Ni_{17}$ (Kelton *et al.* 1997)). The second series was prepared by varying the Co-to-Ni ratio, keeping the Ti and Zr concentrations fixed at that of the best composition for i-(Ti–Zr–Co), namely $Ti_{53}Zr_{27}(Co_{20-x}Ni_x)$. Phase formation and general diffraction features are discussed in this section.

3.1.1. *Ti–Zr–(Fe–Ni) alloys*

The XRD patterns from as-quenched $Ti_{60}Zr_{15}(Fe_{25-x}Ni_x)$ and $Ti_{65}Zr_{10}(Fe_{25-x}Ni_x)$ alloys are shown in figure 1 and figure 2 respectively. For both series, the alloys prepared with a high Ni content contained primarily the i-phase. The prominent i-phase peaks are indexed following the scheme originally proposed by Bancel *et al.* (1985). An increased wheel speed, that is an increased cooling rate, was required to form the i-phase as the Ni concentration decreased $Ti_{60}Zr_{15}(Fe_{25-x}Ni_x)$ alloys over the range $13 \leqslant x \leqslant 25$, indicating a decrease in the i-phase stability with decreasing Ni concentration.

As shown in figure 1, an increase in the wheel speed for alloys containing high Fe concentrations, $0 \leqslant x \leqslant 10$ for $Ti_{60}Zr_{15}(Fe_{25-x}Ni_x)$ did not significantly improve the i-phase formability. There, the Ti_2Ni-type phase (fcc with $a \approx 11.5$ Å) and an ordered bcc β-solid solution phase (from TEM studies) were the dominant phases, with only a small amount of the i-phase present. The i-phase is dominant in $Ti_{65}Zr_{10}Fe_{25}$ (figure 2 (*a*)) and the Ti_2Ni-type fcc is a secondary phase. TEM studies of this alloy show a high density of small i-phase grains, indicating a large nucleation rate. Additionally, crystal approximant phases are found in the alloys prepared with no Ni. These include the M – 1/1 approximant phase (bcc; $a = 13.3$ Å), the λ phase (A face-centred orthorhombic; $a = 32.0$ Å, $b = 26.6$ Å and $c = 10.4$ Å) and the $MgZn_2$-type C14 Laves phase (hcp; $a = 5.15$ Å and $c = 8.37$ Å) (Kim and Kelton 1995).

Electron diffraction patterns taken from the i-phases in the Ti–Zr–Fe alloys contain strong arcs of diffuse scattering and spot shape anisotropy, common for

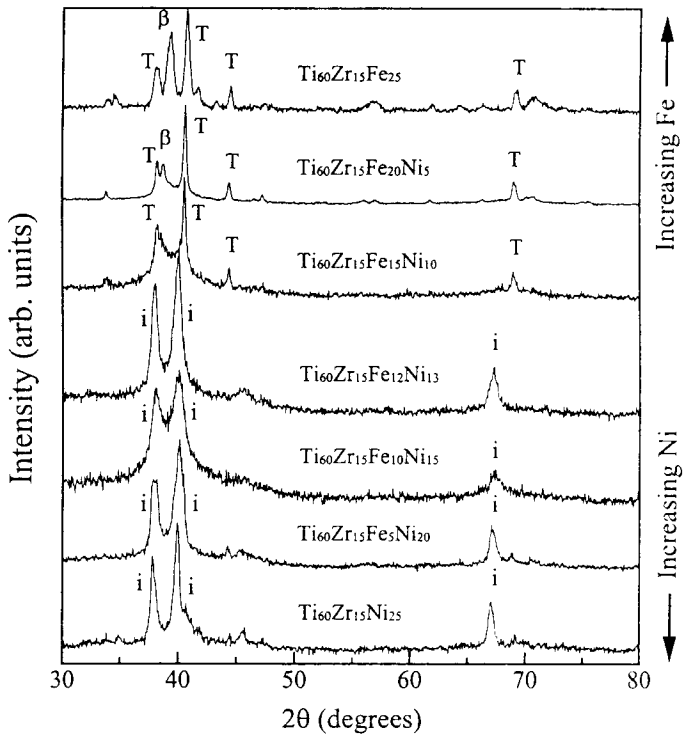

Figure 1. Powder XRD patterns of as-quenched $Ti_{60}Zr_{15}(Fe_{25-x}Ni_x)$ alloys.

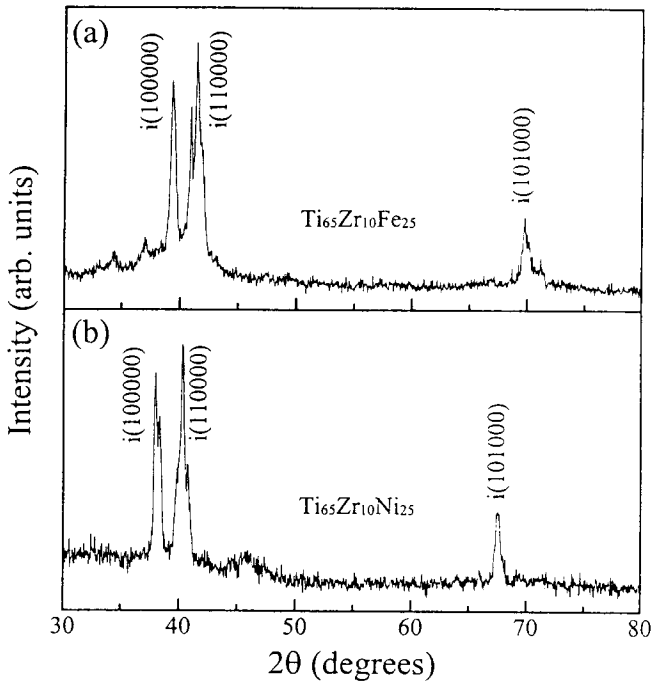

Figure 2. Powder XRD patterns of as-quenched $Ti_{65}Zr_{10}(Fe_{25-x}Ni_x)$ alloys: (*a*) $x = 0$; (*b*) $x = 25$.

the Ti–3d TM–Si i-phases. Studies by Kelton and Gibbons (1992) and Levine and Libbert (1995) indicate that these artefacts arise from topological disorder in the i-phase. These artefacts are less prominent in the high-Ni-concentration alloys ($x > 13$), indicating an increasing structural order of the i-phase. Studies of the ($\bar{\tau}10$) SAD patterns, in which the arcs of diffuse scattering are particularly strong, for the series of alloys showed a monotonic increase in the intensity of diffuse scattering as the Ni was replaced by Fe.

Additional broadening and new peaks in the XRD patterns taken from alloys prepared with no Fe, that is $Ti_{65}Zr_{10}Ni_{25}$ (figure 1) and $Ti_{60}Zr_{15}Ni_{25}$ (figure 2(*b*)), suggest a phase mixture of high-order approximant phases and the i-phase. TEM studies confirm this conclusion. The presence of the high-order approximants probably indicates some Si contamination in the alloys from the SiO_2 quench tube, as discussed earlier by Zhang *et al.* (1994) in $Ti_{53}Zr_{27}Ni_{20}$ alloys.

3.1.2. *Ti–Zr–(Co–Ni) alloys*

The XRD patterns from as-quenched $Ti_{53}Zr_{27}(Co_{20-x}Ni_x)$ alloys are shown in figure 3. Most alloys contain a phase mixture of the i-phase and the C14 hexagonal Laves phase. In contrast with the Ti–Zr–(Fe, Ni) alloys, the Ti_2Ni-type phase is less prominent. The C14 Laves phase forms more readily with increasing Co, making a higher quenching rate necessary to obtain the i-phase (obtained by increasing the wheel speed from 30 to 70 m s^{-1}), indicating a decreasing tendency for i-phase formation. These results suggest that the i-phase is less stable relative to the crystalline approximant phases in the Ti–Zr–Co alloys, compared with Ti–Zr–Ni alloys. This is in agreement with a recent report that a $Ti_{41.5}Zr_{41.5}Ni_{17}$ i-phase is thermodynamically stable (Kelton *et al.* 1997).

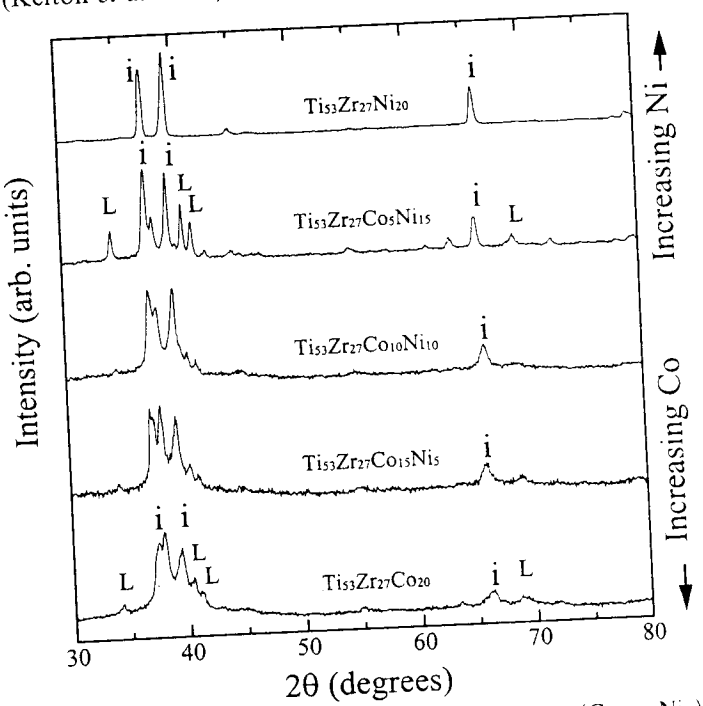

Figure 3. Powder XRD patterns of as-quenched $Ti_{53}Zr_{27}(Co_{20-x}Ni_x)$ alloys.

Electron diffraction patterns taken from i-(Ti–Zr–Co) show weaker spot shape anisotropy and much fainter arcs of diffuse scattering than for those taken from i-(Ti–Zr–Fe). This suggests a greater structural order for i-(Ti–Zr–Co) than for i-(Ti–Zr–Fe). The artefacts become even less visible with increasing Ni and disappear as the Co is completely replaced by Ni, to form $Ti_{53}Zr_{27}Ni_{20}$.

3.2. *Quasilattice constants as a function of alloy composition*

The quasilattice constants as a function of composition were obtained from the X-ray peak positions of the i-phase. As discussed in §3.1, because of the predominant i-phase formation, this was possible for all compositions of the $Ti_{53}Zr_{27}(Co_{20-x}Ni_x)$, for $x = 0$ and 25 in the $Ti_{65}Zr_{10}(Fe_{25-x}Ni_x)$ alloys and for $13 \leqslant x \leqslant 25$ in the $Ti_{60}Zr_{15}(Fe_{25-x}Ni_x)$ series. For values of x outside this range in the $Ti_{60}Zr_{15}(Fe_{25-x}Ni_x)$ alloys, the quasilattice constant was computed from the measured d values of (100000) and (110000) spots from SAD patterns; values from four or more grains were averaged to improve the statistics. The typical variation in the values for the quasilattice constant is about 0.01 Å from the X-ray determinations and 0.02 Å from the SAD measurements. Although, as mentioned, the broad X-ray peaks for the $Ti_{60}Zr_{15}Ni_{25}$ and $Ti_{65}Zr_{10}Ni_{25}$ alloys contained the combined diffraction from the i-phase and high-order approximant phases, the deviation between the expected peak positions of these two phases should be sufficiently small as to have little effect on the tendency of quasilattice constant with alloy composition. The Ni concentration assumed for the abscissa of figures 4 and 5 was obtained from energy-dispersive X-ray spectroscopy in the transmission electron microscope: the error in composition is approximately 2 at.%.

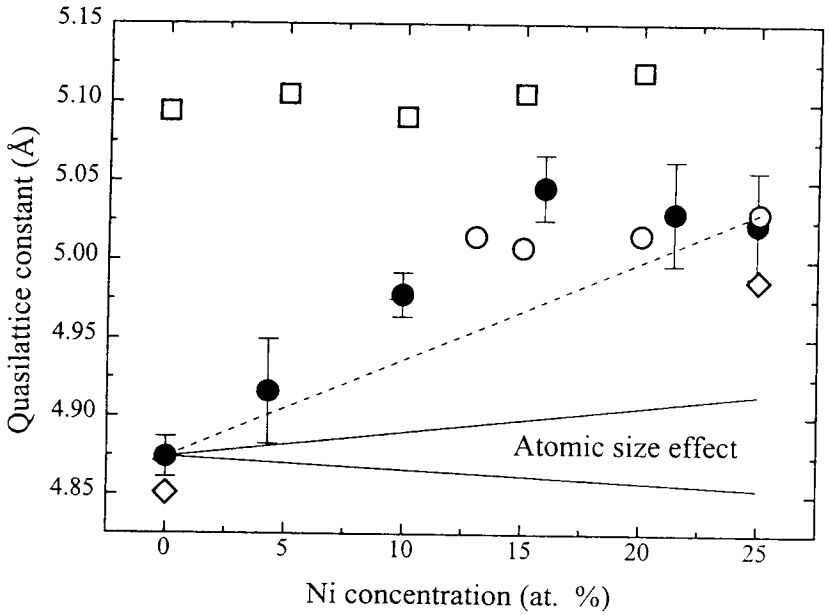

Figure 4. Quasilattice constant as a function of Ni concentration in $Ti_{60}Zr_{15}(Fe_{25-x}Ni_x)$ alloys ((○), from XRD; (●), from SAD), in $Ti_{65}Zr_{10}(Fe_{25-x}Ni_x)$ alloys ((◇), from XRD), and in $Ti_{53}Zr_{27}(Co_{20-x}Ni_x)$ alloys ((□), from XRD). The change expected from differences in atomic size for Fe and Ni is shown.

3.2.1. *Quasilattice constant change in Ti–Zr–(Fe–Ni) alloys*

The quasilattice constant a_q measured for the $Ti_{60}Zr_{15}(Fe_{25-x}Ni_x)$ i-phases is shown as a function of composition in figure 4. The open circles indicate the values obtained from powder XRD patterns; the values indicated by the full circles were obtained from the SAD patterns. Clearly, a_q is a strong function of the Ni concentration, changing by 3.2% over the composition range, from 4.875 Å for $Ti_{60}Zr_{15}Fe_{25}$ to 5.032 Å for $Ti_{60}Zr_{15}Ni_{25}$. For the low-Ni samples, $x \leqslant 13$, a_q increases more rapidly than expected from a simple rule of mixtures (shown by the broken line in figure 4). By both measurement techniques, $a_q \approx 5.03$ Å, approximately independent of the Ni concentration in the high-Ni alloys ($13 \leqslant x \leqslant 25$). A similar change in a_q upon Ni/Fe substitution is observed for the $Ti_{65}Zr_{10}(Fe_{25-x}Ni_x)$ i-phase (open diamonds in figure 4). The quasilattice constant measured from the XRD patterns changes by 2.8% over the range of Ni concentrations studied, from 4.851 Å in $Ti_{65}Zr_{10}Fe_{25}$ to 4.985 Å in $Ti_{65}Zr_{10}Ni_{25}$, as shown in figure 2.

Such large changes in a_q cannot be explained by the size difference between Fe and Ni. Taking the maximum difference in size between these two atoms reported in the literature (Pearson 1972, Zhang *et al.* 1987, Kittel 1996), a change in a_q of less than 0.5% would be expected (indicated by the labelled area in figure 4). Taken together, the large change in the quasilattice constant, the steady progression of the intensity of diffuse scattering, and the difficulty of i-phase formation in high Fe-concentration alloys suggests a structural difference between i-(Ti–Zr–Fe) and i-(Ti–Zr–Ni). This is supported by recent structural refinements by Kim *et al.* (1997) showing that 1/1 M-(Ti–Zr–Fe) has Mackay-type clusters and lattice constant $a = 13.307$ Å, while 1/1 W-(Ti–Zr–Ni) has Bergman-type clusters and lattice constant $a = 14.317$ Å.

3.2.2. *Quasilattice constant change in Ti–Zr–(Co–Ni) alloys*

As shown in figure 4 (open squares), the quasilattice constant a_q for the $Ti_{53}Zr_{27}(Co_{20-x}Ni_x)$ i-phase, computed from the XRD peaks, is approximately independent of the Ni atomic concentration, $a_q \approx 5.10$ Å. The maximum difference between the values of a_q, 5.120 Å for (Ti–Zr–Ni) and 5.094 Å for i-(Ti–Zr–Co), is only 0.026 Å or approximately 0.5%. This is much smaller than the changes found in the $Ti_{60}Zr_{15}(Fe_{25-x}Ni_x)$ and the $Ti_{65}Zr_{10}(Fe_{25-x}Ni_x)$alloys, 3.2% and 2.8% respectively.

Such a small quasilattice constant change in $Ti_{53}Zr_{27}(Co_{20-x}Ni_x)$ alloys may reflect a structural similarity between the Ti–Zr–Co and Ti–Zr–Ni i-phases. The weak diffuse scattering features in the Ti–Zr–Co i-phases suggest more disorder than in the Ti–Zr–Ni. Further, although 1/1 approximants have been found in Ti–Zr–Co alloys (Kim and Kelton 1996), only an undetectably small amount (by XRD) of the 1/1 phase is present in the alloys. Thus it remains to be seen whether they have the same structure as the Bergman-type 1/1 approximant W-(Ti–Zr–Ni).

3.2.3. *Lattice constant change of Ti_2Ni-type fcc phase in Ti–Zr–(Fe–Ni) alloys*

Since the Ti_2Ni-type fcc phase contains distorted single-shell Mackay icosahedra and because the Fe/Ni will occupy sites in that structure that may have a similar local environment to that in the i-phase, it is useful to examine changes in the lattice constant of this phase with substitutions of Fe for Ni at fixed Ti and Zr. The lattice constants determined from powder XRD studies are shown in figure 5. Some values are determined for as-quenched samples (full circles), while others are determined

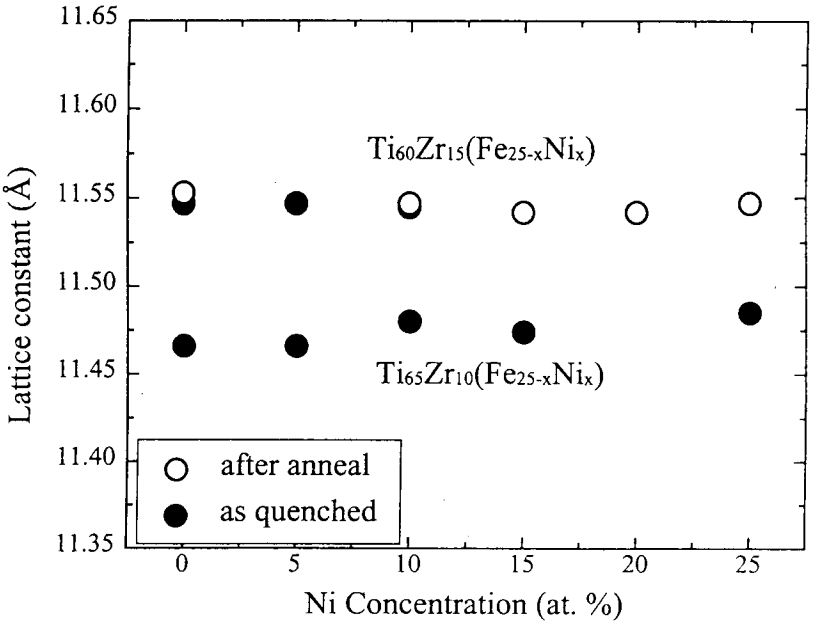

Figure 5. Lattice constant of the Ti_2Ni-type fcc phase as a function of Ni concentration in $Ti_{60}Zr_{15}(Fe_{25-x}Ni_x)$ and $Ti_{65}Zr_{10}(Fe_{25-x}Ni_x)$ alloys.

from annealed samples that transform to the Ti_2Ni phase (open circles). Interestingly, little change is observed with changing Ni concentration; $a \approx 11.547 \pm 0.005$ Å for $Ti_{65}Zr_{15}(Fe_{25-x}Ni_x)$ and $a \approx 11.475 \pm 0.010$ Å for $Ti_{60}Zr_{10}(Fe_{25-x}Ni_x)$ for all concentrations. The maximum deviation from these values over the entire range of Ni concentration is 0.010 Å (less than 0.1%) for $Ti_{60}Zr_{15}(Fe_{25-x}Ni_x)$ and 0.02 Å (less than 0.2%) for $Ti_{65}Zr_{10}(Fe_{25-x}Ni_x)$. These changes, much smaller than the changes in quasilattice constant for the i-phases in Ti–Zr–(Fe-Ni) alloys and the changes in lattice constant between the Ti–Zr–Fe and Ti–Zr–Ni 1/1 phases, are comparable with the changes in a_q for the Ti–Zr–(Co-Ni) alloys and are consistent with the atomic size differences for Fe and Ni.

These results indicate that the sites in the fcc phase for Fe and Ni are sufficiently large and have similar chemistry that free replacement is possible without significantly affecting the local atomic structure. Further they support the argument that, if the Ti–Zr–Fe and Ti–Zr–Ni i-phases are constructed from the same fundamental clusters, little change in the quasilattice constant should be expected with Fe or Ni substitution, as is the case in Ti_2Ni-type fcc structures. Apparently these quasicrystals are not structurally similar, despite the similarity in the chemistries of their components. That their 1/1 approximants contain Mackay and Bergman atomic clusters respectively and differ in their lattice constants by 7% support this conclusion.

3.3. *Classification of quasicrystals*

Two related schemes for the classification of quasicrystals have been suggested. A method proposed by Henley (1986) is based on the ratio between the quasilattice constant a_q, and the expected average atomic distance, calculated from closely

elated crystalline phases. A method proposed by Chen *et al.* (1987) is similar, although it used the average Goldschmidt diameter $\langle a \rangle$. By both methods, most of the Al-based i-phases known at the time of those publications divide into two groups: one related to the crystal 1/1 Bergman phase (Audier *et al.* 1988) and the other related to the 1/1 phase based on the double-shell Mackay icosahedra. By the method of Chen *et al.*, $a_q/\langle a \rangle \approx 1.65$ for the Mackay-type icosahedral phases, characterized by i-(Al–Mn–Si), while $a_q/\langle a \rangle \approx 1.75$ for the Bergman-type quasicrystals, characterized by i-(Al–Li–Cu) and i-(Al–Mg–Zn).

Table 1 presents a more complete compilation of values of $a_q/\langle a \rangle$ that includes additional Al-based quasicrystals to those originally considered and also includes, for the first time, the Ti-based quasicrystals. The quantities a_q and $\langle a \rangle$ for each i-phase are plotted in figure 6. In agreement with the original observations, most i-(Al–TM) phases have smaller quasilattice constants and smaller values of $a_q/\langle a \rangle$, between 1.63 and 1.67; most Al–Li–TM and Al–Mg–TM i-phases have larger qua-

Table 1. Values for selected i-phases giving (from left to right): the number code used in figure 6, the i-phase composition, the quasilattice constant a_q, the average Goldschmidt diameter $\langle a \rangle$, the ratio $a_q/\langle a \rangle$, the reference for the alloy composition and quasilattice constant.

Alloy number in figure 6	i-phase composition	Quasilattice constant a_q (Å)	Average Goldschmidt diameter $\langle a \rangle$	$a_q/\langle a \rangle$	Reference
1	$Al_{5.9}Li_3Cu_1$	5.04	2.905	1.735	Chen *et al.* (1987)
2	$Al_6Li_3Cu_{0.8}Au_{0.2}$	5.07	2.912	1.741	Chen *et al.* (1987)
3	$Al_6Li_3Au_1$	5.13	2.922	1.756	Chen *et al.* (1987)
4	$Al_{51}Li_{32}Zn_{17}$	5.13	2.938	1.746	Chen *et al.* (1987)
5	$Al_6Mg_4Cu_1$	5.17	2.958	1.748	Chen *et al.* (1987)
6	$Al_2Mg_3Zn_3$	5.20	2.952	1.762	Chen *et al.* (1987)
7	$Al_{50}Mg_{35}Ag_{15}$	5.25	2.984	1.759	Chen *et al.* (1987)
8	$Zn_{52}Mg_{32}Ga_{16}$	5.11	2.915	1.753	Chen *et al.* (1987)
9	$Zn_{50}Mg_{42}Y_8$	5.20	3.009	1.728	Elser *et al.* (1996)
10	$Al_{77.5}Mn_{22.5}$	4.58	2.825	1.621	Chen *et al.* (1987)
11	$Al_{82}Mn_{18}$	4.595	2.832	1.623	Chen *et al.* (1987)
12	$Al_{74}Mn_{15}Fe_5Si_6$	4.59	2.805	1.636	Chen *et al.* (1987)
13	$Al_{74}Mn_{20}Si_6$	4.61	2.812	1.639	Chen *et al.* (1987)
14	$Al_{84.5}Cr_{15.5}$	4.66	2.822	1.651	Chen *et al.* (1987)
15	$Al_{60}Cr_{20}Si_{20}$	4.60	2.763	1.665	Chen *et al.* (1987)
16	$Al_{82.5}V_{17.5}$	4.73	2.83	1.671	Chen *et al.* (1987)
17	$Al_{65}Cu_{20}Fe_{15}$	4.452	2.749	1.619	Tsai *et al.* (1987a)
18	$Al_{75}Cu_{15}V_{10}$	4.594	2.797	1.642	Tsai *et al.* (1987b)
19	$Al_{65}Cu_{20}Ru_{15}$	4.53	2.773	1.634	Tsai *et al.* (1988)
20	$Al_{70}Pd_{20}Mn_{10}$	4.562	2.820	1.618	Boudard *et al.* (1992)
21	$Ti_{57}V_{27}Si_{16}$	4.72	2.822	1.673	Zhang and Kelton (1991)
22	$Ti_{60}Cr_{32}Si_8$	4.78	2.807	1.703	Libbert (1995)
23	$Ti_{60}Mn_{37}Si_3$	4.77	2.842	1.678	Libbert (1995)
24	$Ti_{68}Fe_{26}Si_6$	4.77	2.813	1.696	Libbert (1995)
25	$Ti_{60}Zr_{15}Fe_{25}$	4.875	2.874	1.696	Kim and Kelton (1995)
26	$Ti_{65}Zr_{10}Fe_{25}$	4.851	2.861	1.696	Kim and Kelton (1995)
27	$Ti_{53}Zr_{27}Co_{20}$	5.094	2.892	1.761	Kim and Kelton (1996)
28	$Ti_{45}Zr_{38}Ni_{17}$	5.20	2.961	1.756	Stroud (1996)
29	$Ti_{53}Zr_{27}Ni_{20}$	5.12	2.918	1.755	Stroud (1996)
30	$Ti_{60}Zr_{15}Ni_{25}$	5.032	2.864	1.757	This work
31	$Ti_{65}Zr_{10}Ni_{25}$	4.982	2.851	1.747	This work
32	$Zr_{70}Ni_{12}Cu_{11}Al_8$	5.395	3.048	1.770	Köster *et al.* (1996)

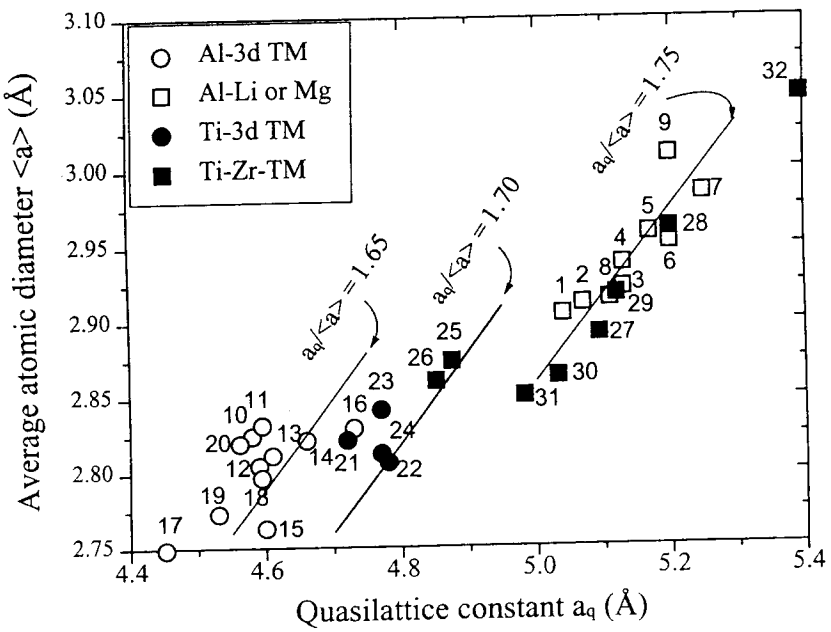

Figure 6. Classification of Al- and Ti-based i-phases using the method proposed by Chen *et al.* (1987), showing the average atomic diameter (calculated from the Goldschmidt radius) against the measured quasilattice constant. Three types of structures are indicated. The values used are listed in table 1, numbered there as in this figure.

silattice constants and larger $a_q/\langle a\rangle$ ratios, between 1.74 and 1.76. The Ti–TM–Si–O i-phases, however, have intermediate quasilattice constants and $a_q/\langle a\rangle$ ratios, between 1.67 and 1.71. This is somewhat surprising since, based on the prominence of the Mackay 1/1 approximant, α-(Ti–Cr–Si–O) (Libbert *et al.* 1994), in these alloys and the similar formation conditions between the i-phase and the α-phases, these i-phases are believed to be of the Mackay type. It may reflect differences in the atomic structures of the i-phases that are similar to those in the relevant 1/1 approximant phases. The approximant α-(Al–Mn–Si) contains 138 atoms, is primitive cubic and has a vacant centre for the Mackay icosahedron; α-(Ti–Cr–Si–O) contains 146 atoms, is bcc, has an occupied centre in the Mackay icosahedron and contains a significant amount of interstitial O. The Ti–Zr based i-phases i-(Ti–Zr–Ni) and i-(Ti–Zr–Co), which are believed to be Bergman-type quasicrystals, group with the Al-based Bergman-type i-phases. Their ratio $a_q/\langle a\rangle \approx 1.75$ appears to be unaffected by the change in alloy system. Among all the Ti–Zr-based i-phases, only i-(Ti–Zr–Fe) falls into the same class as the Ti–TM–Si–O quasicrystals. i-(Ti–Zr–Fe) shows diffraction features that are also most similar to those of i-(Ti–TM–Si–O), and their 1/1 approximants contain similar Mackay-type atomic clusters.

Since the average Goldschmidt diameter is independent of the structure, its relevance to a classification method for quasicrystals is unclear. A scheme is needed that uses more realistic atomic sizes in the structure of interest. We therefore propose here a new scheme based on the ratio between the quasilattice constant a_q and the average atomic separation $\langle a_s\rangle$ computed from the measured mass density ρ. This is a better measure of the average atomic separation, different, for example for two phases with similar chemical compositions but different densities.

Published values for the densities of the i-phases were used when these were available. When not available, they were measured by Archimedes weighing, following a standard procedure described elsewhere (McKinney 1957) and the uncertainty in the densities is less than 1% of the density values in most cases. The average atomic separation was computed from the density ρ as

$$\langle a_s \rangle = \left(\frac{\langle A_w \rangle N_v}{\rho} \right)^{1/3},$$

where N_v is Avogadro's number per mole and $\langle A_w \rangle$ is the weighted atomic mass, that is

$$\langle A_w \rangle = \sum_i x_i A_w^i.$$

Here x_i is the atom fraction of the ith atom and A_w^i is its atomic mass. Although these equations are strictly valid only for sc structures, they allow a reasonable comparison to be made of the fundamental lengths in similar structures. O, required for the formation of the 1/1 α phase and i-phase in Ti–TM–Si–O alloys, occupies only interstitial sites in the α phase, and the lattice constant of the α phase has the same relation with the quasilattice constant of the i-phase that is expected in systems without O. This occurs even though the O concentration in the two phases differs (Libbert *et al.* 1994, Kim *et al.* 1998a,d). O is not believed to change the average atomic separation between metal atoms significantly. In those alloys, the total number of atoms, including the O atoms, was computed from the measured density. The O atoms were subtracted from the total, however, and a metal-atom density was recomputed. These corrected values ρ' and $\langle A_w \rangle'$, computed from only the metal atoms, were then used to compute the average metal-atom separation $\langle a_s \rangle$.

The number, i-phase composition, quasilattice constant a_q, density ρ, calculated average atomic separation $\langle a_s \rangle$ and ratio $a_q/\langle a_s \rangle$ are listed in table 2. Owing to the lack of data for the i-phase density, only representatives of the different i-phase classes are shown; some i-phases listed in table 1 are not listed in table 2. The correlation between the ratio of the quasilattice constant to the average atomic separation $a_q/\langle a_s \rangle$ and $\langle a_s \rangle$ is shown in figure 7. As with the method of Chen *et al.* (1987, figure 6), three distinct groups are recognized, placing the results of that classification method on a firmer physical footing, since the fundamental lengths used are now obtained more directly from the measured density.

All Bergman-type i-phases are grouped near a ratio of $(a_q/\langle a_s \rangle) \approx 2$, suggesting that the structures of these Ti- and Al-based i-phases are very similar. The ratios for the Al-based Mackay-type icosahedral phases lie in the range 1.80–1.85. In contrast, the ratios for the Ti-based Mackay-type i-phases are higher, lying between 1.91 and 1.93, again suggesting different atomic configurations of the two types of Mackay-icosahedron-based quasicrystal. As already discussed, the structures of the two related 1/1 Mackay-based rational approximants are also different, with filled sites in α-(Ti–Cr–Si–O) that are unfilled in α-(Al–Mn–Si). An adjustment of the average atomic separation of the i-(Al–Mn–Si)-type quasicrystals was made by filling sites known to be filled in α-(Ti–Cr–Si–O) and believed to be filled in i-(Ti–Cr–Si–O). This did not move the $a_q/\langle a_s \rangle$ ratios to the higher values found for i-(Ti–TM–Si–O). This indicates that the differences between the two quasicrystals are more significant than this simple difference. The i-phase structures may therefore differ more than their crystal approximants do.

Table 2. Values for selected i-phases giving (from left to right) the number code used in figure 7, the i-phase composition, the quasilattice constant a_q, the density ρ, the calculated atomic separation $\langle a_s \rangle$, the ratio $a_q/\langle a_s \rangle$ and the reference for the alloy composition, quasilattice constant and density. The i-phases listed in table 1 for which densities have not been published are not included in table 2. The fractional uncertainties in the densities are less than 1% in most cases, and the uncertainties in the quasilattice constants are about 0.01 Å

Alloy number in figure 7	i-phase composition	Quasilattice constant a_q (Å)	Density ρ ($g\,cm^{-3}$)	Atomic separation $\langle a_s \rangle$ (Å)	$a_q/\langle a_s \rangle$	References
1	$Ti_{60}Cr_{32}Si_4(SiO_2)_4$	4.78	5.379	2.472	1.934	This work
2	$Ti_{60}Mn_{37}(SiO_2)_3$	4.77	5.413	2.499	1.909	This work
3	$Ti_{65}Zr_{10}Fe_{25}$	4.851	5.551	2.531	1.916	This work
4	$Ti_{60}Zr_{15}Fe_{12}Ni_{13}$	5.015	5.845	2.526	1.985	This work
5	$Ti_{60}Zr_{15}Fe_{10}Ni_{15}$	5.008	5.899	2.519	1.988	This work
6	$Ti_{60}Zr_{15}Ni_{25}$	5.03	5.937	2.158	1.998	This work
7	$Ti_{53}Zr_{27}Ni_{20}$	5.12	6.148	2.555	2.004	This work
8	$Ti_{45}Zr_{38}Ni_{17}$	5.20	6.031	2.631	1.976	This work
9	$Ti_{53}Zr_{27}Co_{20}$	5.094	6.033	2.571	1.981	This work
10	$Al_{86}Mn_{14}$	4.59	3.287	2.514	1.826	Kelton and Wu (1985)
11	$Al_{70}Pd_{20}Mn_{10}$	4.562	5.1	2.459	1.855	Boudard *et al.* (1992)
12	$Al_{62}Cu_{25.5}Fe_{12.5}$	4.464	4.57	2.439	1.830	Elser (1996)
13	$Al_{56}Li_{32}Cu_{11}$	5.04	2.47	2.547	1.979	Janot (1992)
14	$Al_{20}Mg_{40}Zn_{40}$	5.2	3.705	2.641	1.969	Matsuda *et al.* (1990)
15	$Al_{54}Mg_{40}Cu_6$	5.17	2.52	2.652	1.949	Mizutani *et al.* (1990)
16	$Al_{50}Mg_{35}Ag_{15}$	5.23	3.375	2.658	1.968	Mizutani *et al.* (1990)
17	$Zn_{46}Mg_{34}Ga_{20}$	5.11	4.87	2.616	1.953	Mizutani *et al.* (1990)
18	$Zn_{50}Mg_{42}Y_8$	5.20	4.34	2.675	1.944	Elser (1996)

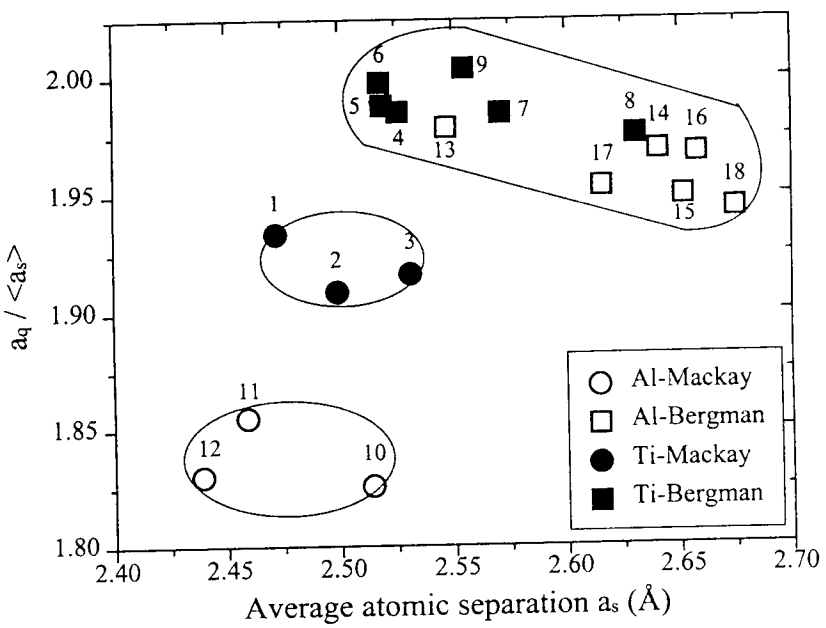

Figure 7. Classification of Al- and Ti-based i-phases using the new method proposed here, showing the ratio of the measured quasilattice constant a_q to the average atomic separation (calculated from the measured density) $\langle a_s \rangle$, against $\langle a_s \rangle$. The values used are listed in table 2, numbered there as in this figure.

The quasilattice constant is generally defined as the edge length of the rhombohedral tiles, which is approximately the distance from the centre to the second-shell vertices of the double-shell Mackay or Bergman clusters in the real materials. Because the nearest atomic separation should approximately equal the distance from the centre to the first-shell vertex of these clusters, $a_a \approx 2\langle a_s \rangle$ was expected and was observed. The small differences among the three families of quasicrystals reflect differences in the ways that their atoms are packed together and are the basis of our classification method.

§4. Conclusions

In summary, i-phase formation was observed over a wide range of Fe/Ni and Co/Ni substitution in rapidly quenched Ti–Zr–(Fe–Ni) and Ti–Zr–(Co–Ni) alloys. The i-phases that form at high Ni concentrations in Ti–Zr–(Fe–Ni) alloys are similar to those found in all Ti–Zr–(Co–Ni) alloys, having similar quasilattice constants and reasonable topological order. In contrast, those formed at high Fe concentrations have smaller quasilattice constants and significant disorder, evidenced by strong localized diffuse scattering and diffraction-spot shape anisotropy. These differences notably arise from differences in the local atomic configurations of these two types of i-phases; their 1/1 approximants contain Mackay-type clusters (Ti–Zr–Fe) and Bergman clusters (Ti–Zr–Ni).

Both a classification method suggested by Chen *et al.* (1987) and a new method introduced by us, correlating the quasilattice constant with an average atomic separation calculated from the measured density, divide the known Al- and Ti-based quasicrystals into three classes:

(1) a Bergman-cluster-based structure that is independent of the primary constituents, that is Ti or Al, and containing i-(Ti–Zr–Ni), i-(Al–Li–Cu) and i-(Al–Mg–Zn);
(2) a Mackay-cluster-based structure for Al-based quasicrystals, containing most of the Al–TM i-phases;
(3) a different Mackay-cluster-based structure for the Ti-based quasicrystals, containing i-(Ti–TM–Si) and i-(Ti–Zr–Fe).

These studies support the inference from the 1/1 approximants of a fundamental difference in structure between the Ti–Zr–Ni quasicrystals (Bergman 1/1 approximant) and the Ti–TM–Si–O quasicrystals, which also include i-(Ti–Zr–Fe) (Mackay 1/1 approximants). They suggest that i-(Ti–Zr–Co) is intermediate between these two extremes, closer to i-(Ti–Zr–Ni), and possibly contains features that occur in both structures.

Acknowledgements

We thank J. L. Libbert and R. M. Stroud for useful discussion. We also thank J. Y. Kim for preparing the $Ti_{60}Mn_{37}(SiO_2)_3$ phase samples. This work was partially supported by the National Science Foundation under grant DMR-92-03052.

References

Audier, M., and Guyot, P., 1986, *Phil. Mag. Lett.*, **53**, L43.
Audier, M., Pannetier, J., Leblanc, M., Janot, C., Lang, J. M., and Dubost, B., 1988, *Physica* B, **153**, 136.

BANCEL, P. A., HEINEY, P. A., STEPHENS, P. W., GOLDMAN, A. I., and HORN, P. M., 1985, *Phys. Rev. Lett.*, **54**, 2422.
BERAHA, L., DUNEAU, M., KLEIN, H., and AUDIER, M., 1998, *Proceedings of the Sixth International Conference on Quasicrystals*, edited by S. Takeuchi and T. Fujiwara (Singapore: World Scientific), p. 207.
BOUDARD, M., BOISSIEU, M., JANOT, C., HERGER, G., BEELI, C., NISSEN, H.-U., VINCENT, H., IBBERSON, R., AUDIER, M., and DUBOIS, J. M., 1992, *J. Phys.: condens. Matter*, **4**, 10149.
BRESSON, L., QUIVY, A., FAUDOT, F., QUIQUANDON, M., and CALVAYRAC, Y., 1998, *Proceedings of the Sixth International Conference on Quasicrystals*, edited by S. Takeuchi and T. Fujiwara (Singapore: World Scientific), p. 211.
CHEN, H. S., PHILIPS, J. C., VILLARS, P., KORTAN, A. R., and INOUE, A., 1987, *Phys. Rev.* B, **35**, 9326.
ELSER, V., 1985, *Phys. Rev.* B, **32**, 4892; 1996, *Phil. Mag.* B, **73**, 641.
ELSER, V., and HENLEY, C. L., 1985, *Phys. Rev. Lett.*, **55**, 2883.
HENLEY, C. L., 1986, *Phil. Mag.* B, **53**, L59.
JANOT, C., 1992, *Quasicrystals, A Primer* (Oxford University Press), p. 152.
KELTON, K. F., and GIBBONS, P. C., 1992, *Phil. Mag.* B, **66**, 639.
KELTON, K. F., GIBBONS, P. C., and SABES, P. N., 1988, *Phys. Rev.* B, **39**, 7810.
KELTON, K. F., KIM, W. J., and STROUD, R. M., 1997, *Appl. Phys. Lett.*, **70**, 3230.
KELTON, K. F., and WU, T. W., 1985, *Appl. Phys. Lett.*, **46**, 1059.
KIM, J. Y., LIBBERT, J. L., and KELTON, K. F., 1998a, *Phil. Mag.* A (submitted).
KIM, W. J., GIBBONS, P. C., and KELTON, K. F., 1997, *Phil. Mag. Lett.*, **76**, 199; 1998b, *Proceedings of the Sixth International Conference on Quasicrystals*, edited by S. Takeuchi and T. Fujiwara (Singapore: World Scientific), p. 47.
KIM, W. J., GIBBONS, P. C., KELTON, K. F., and YELON, W. B., 1998c, *Phys. Rev.* B (in the press).
KIM, W. J., and KELTON, K. F., 1995, *Phil. Mag.* **72**, 1397; 1996, *Phil. Mag. Lett.*, **74**, 439.
KIM, J. Y., SCHILLING, J. S., and KELTON, K. F., 1998d, *Solid State Commun.*, **105**, 551.
KITTEL, C., 1996, *Introduction to Solid State Physics*, seventh edition (New York: Wiley), p. 78.
KÖSTER, U., MEINHARDT, J., ROOS, S., and LIEBERTZ, H., 1986, *Appl. Phys. Lett.*, **69**, 179.
LEVINE, L. E., and LIBBERT, J. L., 1995, *Phil. Mag. Lett.*, **71**, 213.
LIBBERT, J. L., 1995, PhD Thesis, Washington University.
LIBBERT, J. L., KELTON, K. F., GOLDMAN, A. I., and YELON, W. B., 1994, *Phys. Rev.* B, **49**, 11675.
MATSUDA, T., OHARA, I., SATO, H., OHASHI, S., and MIZUTANI, U., 1989, *J. Phys.: condens. Matter*, **1**, 4087.
MCKINNEY, J. E., 1957, *American Institute of Physics Handbook*, third edition (New York: McGraw-Hill), pp. 2–149.
MIZUTANI, U., SAKABE Y., and MATSUDA, T., 1990, *J. Phys.: condens. Matter*, **2**, 6153.
MOLOKANOV, V. V., and CHEBOTNIKOV, V. N., 1990, *J. non-crystalline Solids*, **117–118**, 789.
PEARSON, W. B., 1972, *The Crystal Chemistry and Physics of Metals and Alloys* (New York: Wiley), pp. 155ff.
SAINFORT, P., DUBOST, B., and DUBUS, A., 1985, *C.r. Acad. Sci., Paris*, **10**, 689.
SHECHTMAN, D., BLECH, I. A., GRATIAS, D., and CAHN, J. W., 1984, *Phys. Rev. Lett.*, **53**, 1951.
STROUD, R. M., 1996, PhD Thesis, Washington University.
TSAI, A. P., INOUE, A., and MASUMOTO, T., 1987a, *Jap. J. Appl. Phys.*, **26**, L1505; 1987b, *ibid.*, **26**, L1994; 1988, *ibid.*, **27**, L1587; 1989, *Mater. Trans. Japan Inst. Metals*, **30**, 666.
ZHANG, S. B., COHEN, M. L., and PHILLIPS, J. C., 1987, *Phys. Rev.* B, **36**, 5861.
ZHANG, X., and KELTON, K. F., 1990, *Phil. Mag. Lett.*, **62**, 265; 1991, *ibid.*, **63**, 39.
ZHANG, X., STROUD, R. M., LIBBERT. J. L., and KELTON, K. F., 1994, *Phil. Mag.* B, **70**, 927.